Polyanions in liquid ionic alloys: a decade of research

1996 J. Phys.: Condens. Matter 8 6115

(http://iopscience.iop.org/0953-8984/8/34/003)

J. Phys.: Condens. Matter **8** (1996) 6115–6138. Printed in the UK

REVIEW ARTICLE

Polyanions in liquid ionic alloys: a decade of research

W van der Lugt

Solid State Physics Laboratory, University of Groningen, Nijenborgh 4, 9747 A G Groningen, The Netherlands

Received 20 February 1996, in final form 20 May 1996

Abstract. The occurrence of polyanions in a group of liquid ionic alloys, *viz.* alloys of the alkali metals with 13, 14, 15 and 16 elements (post-transition-metal groups 3, 4, 5 and 6), is discussed. It is shown that there are strong parallels with the corrresponding crystalline phases, in which polyanions such as $(Pb_4)^{4-}$, $(Sb^-)_\infty$ and $(Te_2)^{2-}$ exist, known for a long time as 'Zintl ions'. Little evidence exists for remnants of the diamond-lattice-type Zintl ion in liquid alkali–group-13 alloys, but in the alloys of Tl with K, Rb and Cs very long-range superstructures have been found, which are related to the occurrence of large, compact, polyhedral clusters in many crystalline phases.

A stability rule, first proposed by Geertsma, relating the stability of the polyanions to the size of the cations, is universally observed. Furthermore it is shown that the range of the superstructure in the liquid is with remarkable precision proportional to the intercluster distance in the corresponding solids.

The interpretation of the experimental data in terms of polyanion formation is discussed critically. There remains a paradox. Some sharp experimental features (superstructure peaks and maxima in the resistivities and stability functions) seem to indicate that the Zintl ions in the liquid are near perfect whereas specific heat results and *ab initio* computer simulations clearly show that the structure of the liquid is seriously blurred.

1. Introduction

This review paper deals with binary liquid alloys of alkali metals with elements of the groups 13, 14, 15 and 16 (post-transition-metal groups 3, 4, 5 and 6), all of them simple s–p alloys. The main driving force behind the phenomena to be discussed is the ionicity: the difference between the electronegatives of the constituents is large and increases with the distance between the respective columns in the periodic table. For KIn it is, on the Pauling scale, 0.96 and for CsSb it is 1.26. On the Miedema scale these numbers are 1.65 and 2.45, respectively. The ionicity explains the formation of saltlike octet compounds such as Li_4Pb in these systems. The occurrence of polyanions in such alloys, which is the subject of this paper, is necessarily accompanied by the formation of *covalent* bonds and therefore their discovery was first met with some surprise.

In the study of these liquid alloys elementary chemical notions play an important role: what is a liquid compound; what is its 'stoichiometric' composition? Even on this level not everything is completely settled and sometimes inconsistencies remain between the indications from different experiments. This is not a field for firm conclusions and precise descriptions but rather for conjectures and crude models. Analogies with the solid-state counterparts provide important arguments for the interpretation of the data.

An important working hypothesis (but without general validity) is that liquid compounds can be detected, and their 'stoichiometric compositions' can be defined, by extrema in the

0953-8984/96/346115+24$19.50

physical properties plotted as a function of composition. An early example of this approach is given in [1]. This hypothesis is obvious for thermodynamic quantities such as the Darken stability $D = (\partial^2 G/\partial c^2)_{p,T,N}$ (where G is the Gibbs free energy and c the fraction of one of the components), the heat and entropy of mixing and the specific heat. It is at least plausible for the electrical resistivity, ρ, as the formation of a compound is usually accompanied by the formation of a (pseudo-) gap or a minimum in the electronic density of states. This can be an ionic gap in the octet compounds or a covalent gap in the clustered compounds. According to their resistivities most of the liquid compounds discussed here can be classified as corresponding to Mott's regime II [2]. With only very few exceptions the temperature derivative of the resistivity, $\mathrm{d}\rho/\mathrm{d}T$, is negative for the compositions conforming to this regime. The minimum in $\mathrm{d}\rho/\mathrm{d}T$ against c occurs at the same composition as the maximum in ρ against c. An example is given in figure 1. The negative sign of $\mathrm{d}\rho/\mathrm{d}T$ can be explained from different points of view: first, in terms of the diffraction model, which predicts a small or negative $\mathrm{d}\rho/\mathrm{d}T$, when $2k_F$ falls under the main peak of the structure factor [3]. Second, with increasing temperature the interval kT sampling states about the Fermi level obviously becomes larger [4]. The third and probably most important mechanism is the gradual break-down of the local ordering with increasing temperature. This local ordering stabilizes the non-metallic state [5]. Allgaier [6], in an old but still informative paper, gave an overview of the behaviour of $\mathrm{d}\rho/\mathrm{d}T$ in liquids. In the present paper we will not be concerned primarily with electronic processes as such. Two pertinent papers are listed as [4] and [7]. Tables with experimental resistivity values for many ionic liquid alloys systems can be obtained from the present author on request.

Also other properties, such as the density, the magnetic susceptibility, χ, and the Knight shift, K, may be used for detecting liquid compounds. Volume contraction is likely to occur when the cations assume a noble-gas configuration. Changes in the electronic density of states at the Fermi level are reflected in the spin paramagnetism and consequently in the Knight shift. The alkali Knight shift decreases strongly upon the addition of the polyvalent metal. This is usually associated with the depletion of the Fermi electron density at the alkali nucleus. Indeed, the Knight shift levels off at compositions where because of valence considerations one might expect the charge transfer to be completed. Moreover, minima occur where the resistivity measurements indicate that the system has entered Mott's regime II and consequently the Fermi density of states decreases below its NFE value [8]. However, this splitting into charge transfer and density-of-states effects is not free from arbitrariness.

A property of special importance for the study of polyanion formation is the spatial structure of the liquid as determined by means of neutron or x-ray diffraction. It gives direct information on the chemical configurations found in the liquid. Therefore such experiments are crucial even for a first exploration of a liquid alloy system. However the interpretation of such data is not entirely unique; it will be shown below that a variety of polyanion configurations can be compatible with an experimental structure factor.

Most of the phase diagrams of our ionic binary systems are fairly complex and contain a considerable number of solid compounds. A typical example is given in figure 2. In contrast, the number of liquid compounds as defined above is only one or two per system, obviously due to the absence of constraints associated with the requirements of a periodic lattice. We will frequently conjecture the persistence of elements of the crystal structure (and, consequently, of the electronic structure) in the liquid. There is some arbitrariness in choosing a solid reference compound for comparison with a liquid mixture. It is intuitively plausible that congruently melting compounds and compounds with a high melting point have the best chances to survive in some form in the liquid, but this is a far from perfectly

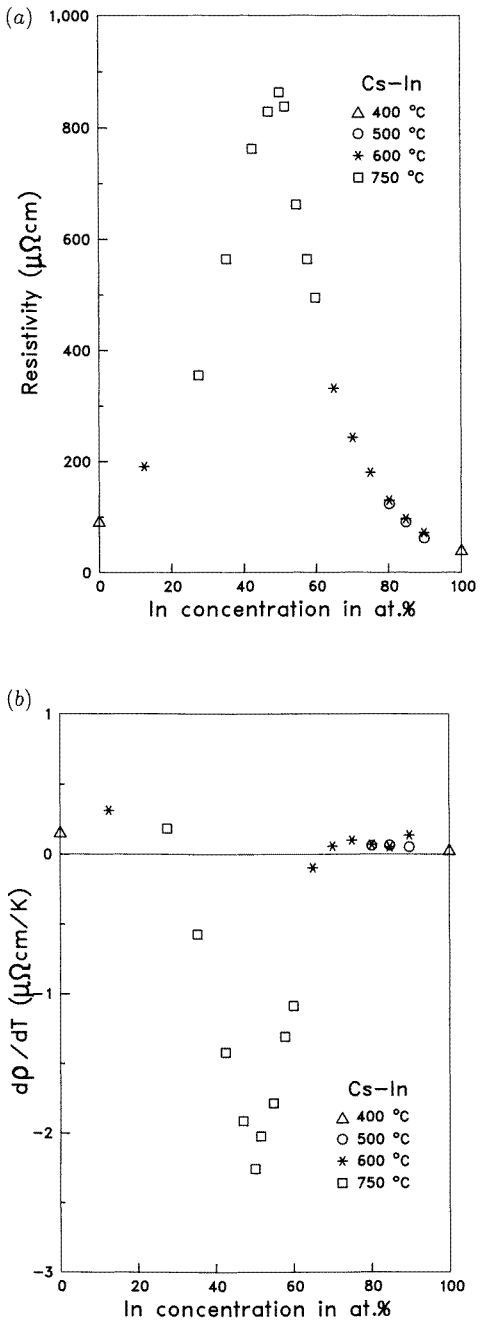

Figure 1. Electrical resistivity (*a*) and its temperature derivative (*b*) for liquid Cs–In alloys as a function of composition and at temperatures in the figure. (Reproduced from [93].)

safe guideline. For instance: it is essential for our discussion below that the congruently melting compound LiPb does *not* show up as a liquid compound.

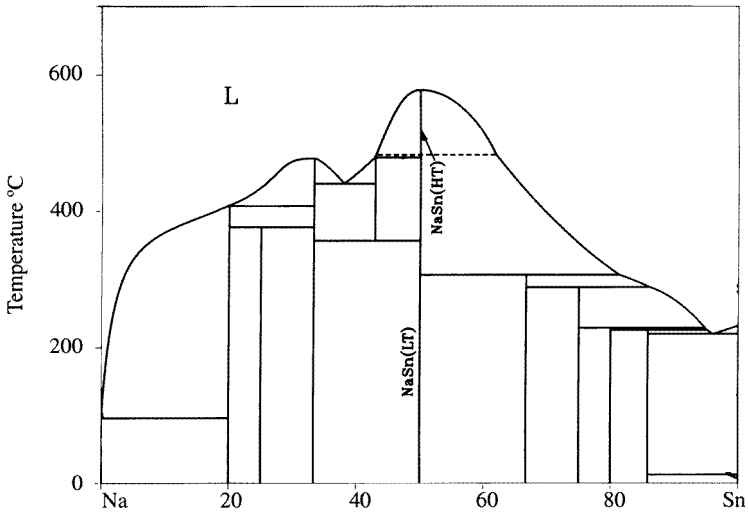

Figure 2. The phase diagram of the Na–Sn system. Liquid compounds are formed at 23 and 43 at.% Sn. (Reproduced, though with drastic modifications, from Massalski T B (ed) 1986 *Binary Alloys Phase Diagrams* (Metals Park, OH: The American Society for Metals).

This article has a larger companion in the form of a chapter in Kauzlarich S M (ed) *Chemistry, Structure and Bonding of Zintl Phases and Ions*, to be published by Chemie [9]. The latter paper addresses primarily crystal chemists. The reader may find there more detailed information, which does not fit within the scope of the present paper. Some earlier review papers are listed as [4], [10], [11] and [12].

As the interpretation of the properties of liquid compounds relies a great deal on comparisons with the crystalline counterparts, the next two sections will be devoted to some aspects of crystal chemistry rather than to the physics of liquid metals.

2. Zintl ions

The solid ionic compounds form a paradise for crystal chemists as they display an astonishing richness in crystal structures, some of them with architectural qualities. A frequent phenomenon is the occurrence of polyanions, negatively charged clusters of the polyvalent metal.

In the discussion of polyanions the concept of 'Zintl ions' plays an important role. Zintl and Woltersdorf [13] noticed that anions tend to form the same cluster geometries as expected for neutral atoms with the same valence electron configuration. A well known example is Pb^-, which occurs in tetrahedral $(Pb_4)^{4-}$ units in all crystalline equiatomic compounds of Pb with Na, K, Rb and Cs (see figure 3). According to the Zintl model $(Pb_4)^{4-}$ is the analogon of the tetrahedral molecules As_4 and P_4. Also the polyanions $(Si_4)^{4-}$, $(Ge_4)^{4-}$ and $(Sn_4)^{4-}$ occur in the respective 50–50 ('equiatomic') alloys with alkali metals. The example considered by Zintl and Woltersdorf [13] was LiAl, in which the Al atoms are situated on a diamond-type lattice, which according to the above-mentioned rule is the (infinitely large) Zintl ion of Al. The Li atoms occupy the 'empty positions' in the diamond lattice, which form a diamond sublattice themselves.

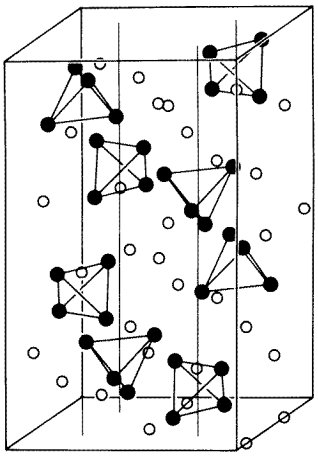

Figure 3. The crystal structure of NaSn. (Reproduced from [20].) Full circles, Sn; empty circles, Na.

Further examinations and discussions of the Zintl principle were given by Busmann [14] and by Klemm and Busmann [15]. Pearson [16] formulated the electron-counting condition

$$[(n_e + b_a - b_c)/n_a] = 8 \tag{1}$$

where n_e is the total number of valence electrons, n_a is the number of anions, b_a is the number of electrons involved in anion–anion bonds and b_c is the number of electrons involved in cation–cation bonds. All these numbers should be calculated per formula unit; b_c is zero for most alloys dealt with in this paper. From this rule, which simply reflects that an atom likes to have eight electrons in its valence shell, one can calculate the anion–anion coordination number. Of course, not all the compounds formed by two elements of the groups considered in this paper can be described as Zintl compounds. We will be mainly concerned with equiatomic binary compounds, in which one electron is (formally) transferred from the more electropositive to the more electronegative atom.

The concept of Zintl ions is in practice not clearly delimited and the term 'Zintl ion' is often used for kinds of polyanion different from the simple examples given above. The electron-counting rules may be different from Pearson's (equation (1)) and are sometimes described in terms of the so-called Wade rules [17] or even in terms of deviations from these rules. These electron-counting rules were originally formulated for boranes and carboranes; they are more complex as they depend on the shape of the molecule or polyanion. As they are of limited use for the discussion in this paper we refer the reader to modern textbooks of inorganic chemistry such as [18].

It is beyond the scope of this article to provide a critical discussion of such extended definitions of Zintl ions. The term 'Zintl ions' will here be reserved for compounds observing Pearson's valence rule. A recent, concise discussion of the Zintl–Klemm concept can be found in the introductory pages of [19], while a more extensive review on Zintl ions is given in [9].

Other examples of Zintl ions are the (infinite) tellurium-like chains for Sb^- and, very straightforwardly, the dumbbells for Te^-, analogons of the halogen molecules. The 'ultimate' Zintl ion is Cl^- in NaCl, occurring isolated in the lattice as expected for a noble gas atom. However the term Zintl ion is never extended to such extreme cases. The

electronegative elements are restricted to the metametals, 'a grey zone in the periodic table, which divides nonmetallic elements from the typical metals' [19].

3. Electronic structure

The Zintl picture requires the formal transfer of a whole number of electrons from the more electropositive to the more electronegative atom. This number does not correspond to the real charge transfer, as determined, e.g., from an electronic-structure calculation. Indeed, the latter quantity is notoriously difficult to define. It is better to say that the wavefunctions of the transferred electrons are governed by the deep electron–ion potentials of the more electronegative atoms.

That this picture is sound was demonstrated by calculations by Springelkamp *et al* [20]. The band structure of NaSn, which contains tetrahedral Zintl ions $(Sn_4)^{4-}$, is remarkably similar to the term schemes of P_4 and As_4 [21, 22], if one imagines the energy levels of the latter to be broadened into bands. The Fermi energy is in a covalent gap between what are essentially the bonding and the antibonding states of $(Sn_4)^{4-}$.

Such tetrahedral units occur in all alloys of Si, Ge, Sn and Pb with Na, K, Rb and Cs, but not in the Li alloys. This observation stimulated Geertsma and coworkers [23] to propose a model for the stability of Zintl ions. He compared the energies of the 'clustered' configuration with a fictive nonclustered configuration, represented by a CsCl lattice. Three interaction parameters, U, V and T, were introduced, representing respectively the anion–anion interaction within a cluster, the anion–anion interaction between two anions forming part of different clusters and the anion–anion interaction in the CsCl structure. Scaling U, V and T with the interatomic distances according to rules of thumb as found e.g. in [24], and substituting the experimentally known interionic distances, he could show that indeed a transition from nonclustered to clustered occurs between Li–B and K–B, B denoting the

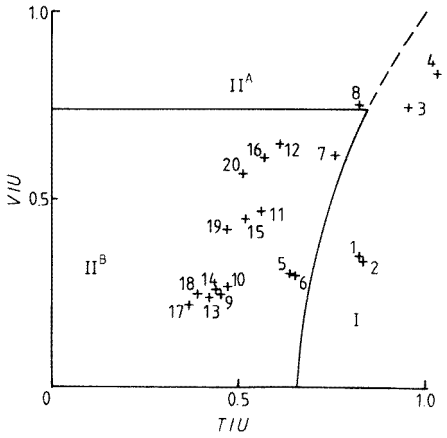

Figure 4. Relative stability of clustered and nonclustered alkali–group-14 compounds: region I, nonclustering; region II^A, clustering, metallic; region II^B, clustering, nonmetallic. The numbers refer to the following systems: 1–4, LiSi–LiPb; 5–8, NaSi–NaPb; 9–12, KSi–KPb; 13–16, RbSi–RbPb; 17–20, CsSi–CsPb. U symbolizes the covalent interaction between anions within a cluster, V that between anions of different clusters and T that between anions in a fictive CsCl structure. (Adopted from [23].)

polyvalent metal atom (figure 4).

According to this model the essential mechanism for the transition is a size effect. Note that the volume of the alkali atoms increases by a factor of five to six from lithium to caesium. In a homogeneous mixture of, say, caesium and lead the caesium atoms push the lead atoms so far apart that the lead–lead interactions are considerably reduced compared to a lithium–lead mixture. It is then more profitable for the lead atoms to cluster together, so that their mutual distances become smaller and the energy of their bonds is reduced.

This model is based on crude approximations such as the complete neglect of ionic interactions, but its validity, at least as an empirical rule, has proven to be remarkably universal and is not restricted to alloys of alkali metals with group-14 elements. In the original paper [23] the theory is formulated in terms of a tight-binding model applied to a pseudolattice. This description is general enough to be equally applicable to crystalline and noncrystalline materials. In the form discussed here, it pertains particularly to compact clusters, but it can be extended to more network-like configurations [25].

An extensive account of the band structures of crystalline alkali–lead alloys has been given by Tegze and Hafner [26]. It nicely illustrates the change in band structures at the transition from nonclustered to clustered configurations.

Calculations by Hart *et al* [27] showed that the bonds in the P_4 molecule are strained, more particularly that electron lobes are protruding from the centres of the tetrahedral faces and along the threefold axes. In the alkali–Pb, Sn alloys such accumulations of charge are favourable positions for the positive alkali ions. In the crystals one finds that half of the alkali atoms are situated opposite the tetrahedral faces such that one alkali atom connects two faces belonging to adjacent tetrahedra. The other half are situated near the threefold axes and connect two vertices (figure 3).

4. Liquid alkali–group-14 alloys

4.1. The 'perfect Zintl model'

Of all the liquid systems dealt with in this paper the alkali–Pb and Sn alloys are those in which polyanion formation has been studied most extensively. The primary observations were the occurrence of a double maximum in the electrical resistivity of liquid Na–Sn [28] and the shift of the position of the resistivity maximum from approximately 20% lead to 50% lead when going from Li–Pb to K–Pb [29]. The maximum remains at 50% for Rb–Pb and Cs–Pb [30], while its value increases rapidly from K–Pb to Cs–Pb. Figure 5 illustrates the resulting difference between Li–Pb and Cs–Pb. Liquid Li–Pb had been studied intensively before [31, 32] and had turned out to be an essentially ionic alloy system with the accompanying Coulombic ordering phenomena. The compound at 20% can be written formally as $Li_4^+Pb^{4-}$ and observes the most elementary form of the octet rule. The behaviour of the alkali–Sn alloys is very similar to that of the alkali–Pb alloys. Na–Pb and Na–Sn are transition cases. This shift of the maximum was related to the congruently melting compounds, which occur in all the corresponding phase diagrams (except for Cs–Sn) at 50% Pb, Sn. As we have seen, in the solid compounds the anions occur as tetrahedral Zintl ions B_4^{4-} and it was supposed that they assume the same configuration in the liquid.

The shift of the stoichiometry has been amply confirmed by measurements of other properties of which we mention in particular the stability function [33, 34], the specific heat [33–35], the density [35, 36] and the Knight shift [37]. The change in stoichiometry in between Li–Pb and K–Pb (and in between Li–Sn and K–Sn) is in perfect agreement with Geertsma's predictions.

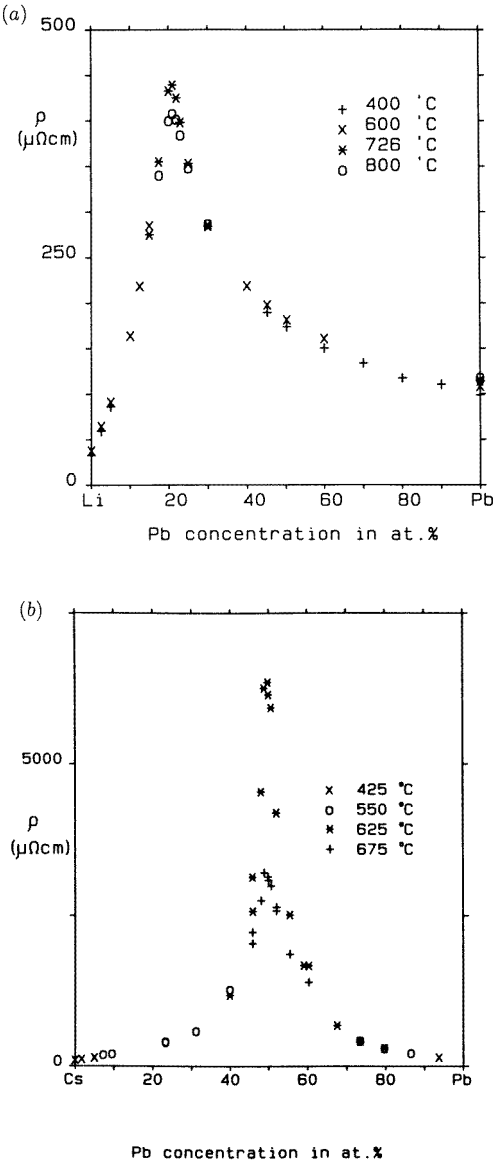

Figure 5. Restivities of liquid Li–Pb (*a*) and Cs–Pb (*b*) alloys as a function of composition at temperatures indicated in the figure. (Reproduced from [29] and [30], respectively.)

Also the observed strong increase of the resistivities from K–Pb to Cs–Pb and from K–Sn to Cs–Sn can be explained within Geertsma's model by noticing that all the electrons which contribute to the conduction are, at least formally, in Pb (Sn) orbitals, and that the transfer integrals between Pb states decrease in magnitude as the distances between the Pb atoms become larger. An equivalent way of phrasing the same physical mechanism is to say that the bands become narrower and consequently the density of states near the Fermi level becomes smaller.

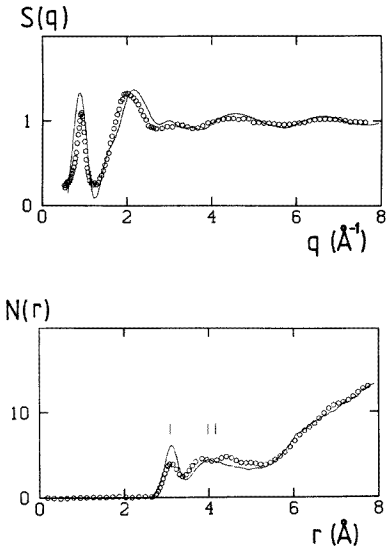

Figure 6. Structure factor and radial distribution function for liquid CsPb: circles, experiment; line, molecular dynamics simulation. (Reproduced from [43].)

Neutron-diffraction measurements (figure 6) of the equiatomic compounds [38, 39] are in agreement with the Zintl picture. There is a high and well resolved prepeak indicating a superstructure, which we identify with the more or less regular arrangement of the tetrahedra. Its wavevector, k_0, should then be related to the average intercluster distance d in the crystal. Indeed, d and k_0 observe approximately the rule of thumb $dk_0 = 7.7$ ([40, 41], see also the last section of this paper). The radial distribution functions each exhibit a peak at a distance equal to the tetrahedral Pb–Pb bond length. Similar experiments have been carried out for alkali–tin alloys [42]. No measurements of the partial structure factors, for instance by means of isotope substitution, have as yet been reported.

To interpret the neutron data essentially two models were proposed. One uses analytical theories of the liquid state [39] and introduces as building blocks neutral entities of the kind $Pb_4^-Cs_4^+$, the Cs^+ ions being positioned opposite the faces of a Pb_4^{4-} tetrahedron and thus forming a larger tetrahedron by themselves, in accordance with the calculations by Hart *et al* [27] (see section 3). We will denote this by the term 'augmented tetrahedron'. The other one [43] uses computer simulation and assumes *a priori* the existence of Pb_4^{4-} tetrahedra, whereas the alkali atoms are allowed to move without such special constraints. Both models are in satisfactory agreement with experiment, though the latter one is distinctly the best. Recently, Stolz *et al* [44] extended the neutron-diffraction experiments on KPb and NaSn to high temperatures and low densities. We concentrate here on KPb. They found that the prepeak survives under these extreme thermodynamic conditions, but that it shifts to lower k-values and becomes broader. This indicates that with increasing temperature the separation of the clusters becomes larger. Indeed the shift of the wavevector is in good agreement with the 25% density decrease observed by the authors. Another indication for the survival of Zintl ions is that the maximum in the radial distribution function at 3.2 Å, which corresponds to the Pb–Pb distance within a tetrahedron, does not change position. We conjecture that the disorder created by the higher temperatures is counteracted by a stabilization of the tetrahedra due to their larger mutual distance: in terms of Geertsma's

model the ratio V/U becomes smaller in the case of cluster formation and T/U would become smaller for the fictive homogeneous case. A glance at figure 4 shows that this leads to stabilization of the clusters.

Diffraction experiments covering the entire composition range [45, 46] showed that for comparisons between 50% and the pure metals the Bhatia–Thornton structure factor $S_{CC}(0)$ (which is inversely proportional to the Darken stability function) becomes large, indicating a tendency to phase separation. This is to be expected when the equiatomic compound is very stable. It is also in agreement with the experimental observation of strong evaporation in the alkali-rich alloys. The structure of the liquid alloys rich in polyvalent metal shows a similarity with the Laves phase found for crystalline KPb_2 [47]: with increasing Pb content the tetrahedra gradually coalesce into larger units, until the pure metal Pb is formed.

4.2. Randomness

So far the 'Zintl model' for liquid alkali–Pb, Sn alloys works remarkably well: it explains the stoichiometries of the experimentally found compounds, there is a theoretical model which accounts for the relative stabilities and structural investigations confirm that elements of the crystal structure survive in the liquid. Note that we could explain everything in terms of a 'perfect Zintl model': tacitly all polyvalent atoms were supposed to be arranged in tetrahedra and we did not bother about possible dissociation and other forms of rearrangement of the anions. This is, of course, not realistic, and we will now discuss some measurements and calculations which cast considerable doubt on this picture.

Measurements of the specific heat as a function of temperature [48] showed, first, that the specific heat just above the melting point is extremely high compared to normal metals; it is plausible to explain this in terms of a blurring of the structure, more particularly a dissociation of the Zintl ions. Second, the specific heat decreases rapidly as a function of temperature, which reflects the completion of this dissociation process. Third, the onset of the decrease shifts to higher temperatures in the sequence K–Pb to Cs–Pb, which is in agreement with our stability considerations.

Howe and McGreevy [49] and Stolz *et al* [50] analysed the structure factors by means of the reverse Monte Carlo method. The main result in [49] is that a large range of atomic configurations, with different degrees of dissociation, appear to be compatible with experiment. [50] contains instructive simulated configurations which exhibit a disorder not dissimilar to that of figure 7. This does not imply that the former interpretation in terms of perfect structural building blocks [39, 43] is wrong (it is in quite reasonable agreement with experiment) but that regarding the question of perfectness of the Zintl ions it is not conclusive [51]. There is simply no more information in the total structure factor and it is questionable whether or not knowledge of the partial structure factors would have resulted in a substantially more concrete picture.

Also *ab initio* molecular dynamics simulations of liquid CsPb resulted in a much more random atomic arrangement than one would expect from the perfect Zintl picture [52, 53]. The tetrahedra are fragmented and fragments have linked up again (see figure 7). The simulation reproduces the structure factor and radial distribution function very nicely. Even the prepeak is in the right position, which is remarkable in view of the relatively small size of the system studied. We therefore believe that the arrangement in figure 7 is quite realistic. Also the partial bond-angle distributions resulting from the simulations are illuminating: the Pb–Pb–Pb distribution exhibits much sharper features than the Cs–Cs–Cs distribution, as expected because of the more covalent interactions between the lead atoms (figure 8). *Ab initio* simulations are at the time being the only way to account for the directed bonds

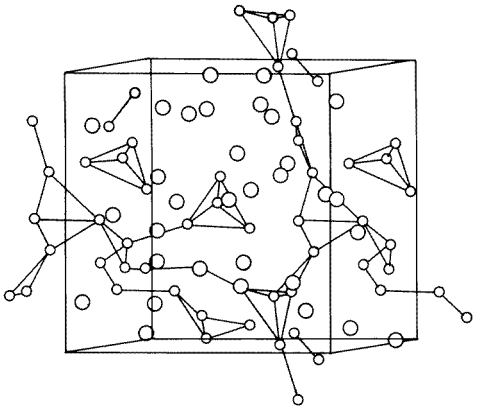

Figure 7. A snapshot of the *ab initio* simulation of liquid CsPb: small circles, Pb atoms; large circles, Cs atoms. Some Pb atoms are hidden behind Cs atoms, so that seemingly Cs atoms form part of the tetrahedra. (Reproduced from [53] with permission from the American Institute of Physics.)

expected in covalent structures. Unfortunately they are restricted to small numbers of particles (typically 100) and rely on the local-density approximation. For other simulations providing insight in the general nature of the bonding we refer the reader to the original literature [54].

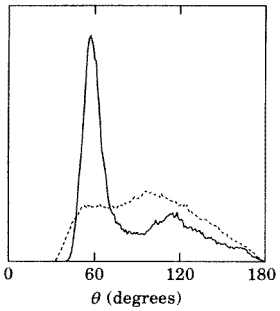

Figure 8. Bond-angle distributions from the *ab initio* simulations for liquid CsPb: full curve, Pb–Pb–Pb; dotted curve, Cs–Cs–Cs. The vertical scale is arbitrary. (Reproduced from [52] with permission from Les Editions de Physique.)

We have now met three models for the equiatomic alkali–Pb, Sn alloys: the 'augmented' Zintl ion Cs_4Pb_4, the model in which $(Pb_4)^{4-}$ polyanions are swimming in a 'fluid' of alkali ions and the more random picture following from the *ab initio* calculations and the reverse Monte Carlo analysis. The latter picture is probably the most realistic one. Intuitively we are left with the paradox that so chaotic an arrangement can be apparently in agreement with sharp experimental features, such as the maxima in so many physical properties and the well resolved superstructure peaks in the structure factors. Obviously the electronic structure and the superstructure in the liquid are not coupled so specifically to perfect Zintl configurations.

4.3. Rotor phases

We make a small digression from the liquids to the high-temperature (HT) solid phases. During the last few years considerable attention has been paid to the dynamics of these phases. The solid Zintl compounds discussed in section 2 are the low-temperature (LT) phases. The HT phase extends from the transition temperature to the melting point (see figure 2).

It can be shown by measurements of the inelastic neutron scattering [55, 56] that the HT phase of CsPb is a plastic crystal (in this case a 'rotor phase'). The spectrum could be modelled by assuming that 'augmented' tetrahedra Cs_4Pb_4 rotate rather freely within the crystal. This is facilitated by the nearly spherical shape of these units. They are also chemically saturated and electrically neutral, so that their mutual bonding relies mainly on Van der Waals forces. Until this discovery, plastic behaviour had not been found in intermetallic phases, but rather in materials such as NH_4Cl and pentaerythritol ($C(CH_2OH)_4$).

In the HT phase of NaSn, the simple tetrahedra $(Sn_4)^{4-}$ rotate and, by means of a 'paddlewheel' mechanism, are responsible for enhancing the 'jump' (translational) migration of Na^+ ions ([57, 58], see also figure 9). The analysis of electrical transport properties of plastic CsPb and NaSn suggests that there is a strong influence of the mobile ions on the electron states: both the energy gap and the mobility are affected. This could possibly be a novel mechanism, beyond the adiabatic approximation [59].

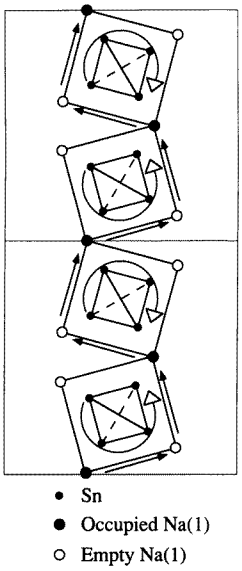

Figure 9. A schematic picture of the paddlewheel mechanism for ion diffusion in plastic NaSn. (Figure reproduced from [58].)

It is remarkable that the HT phases appear to have a lower symmetry than the LT phases. For a more disordered, liquid-like structure the opposite is expected. A review of these rotor phases is given in [60].

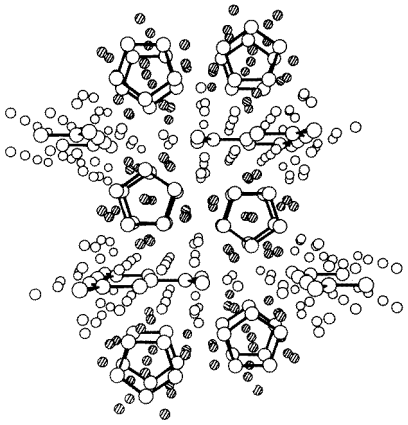

Figure 10. A perspective view of the crystal structure of $Li_{12}Si_7$. (Reproduced from [61] with permission from the publishers of *Berichte der Bunsengesellschaft.*)

4.4. Li–Si and Li–Ge

Very little is known about the liquid alloys of Na, K, Rb and Cs with Si and Ge, probably because of experimental problems. As expected from figure 4 the lithium alloys do not form tetrahedral Zintl ions, but a variety of other fascinating crystal structures exists in the alkali-rich compounds. An example is given in figure 10 for the composition $Li_{12}Si_7$. It contains five-membered rings and four-membered stars [61]. So the question arises: what is left of such beautiful structures in the liquid?

The resistivities of Li–Pb, Li–Sn, Li–Ge and Li–Si exhibit a distinct trend [62]. For Li–Pb and Li–Sn there are only the octet peaks. Then for Li–Ge the peak broadens on the Ge-rich side and has a little hump at 43% Ge. For Li–Si the resistivity curve, after an initial rise to approximately 650 $\mu\Omega$ cm, is essentially flat beyond 20% Si. The Knight shift and spin–lattice relaxation time exhibit an analogous behaviour.

We focus attention of $Li_{12}Si_7$ and its liquid counterpart $Li_{65}Si_{35}$. Neutron-diffraction measurements were carried out by De Jong *et al* [63, 64]. According to an analysis by the reverse Monte Carlo method the Si–Si–Si bond-angle distribution exhibits, apart from the usual sharp maximum at 60°, a very broad and low maximum at higher angles, covering both 108 and 120° corresponding to the angles in the fivefold rings and the stars, respectively. However, more generally no evidence is found for the survival in the liquid of particular structural elements existing in the solid. A variety of Si aggregates with twofold-, threefold- and fourfold-coordinated Si atoms is formed, in agreement with the suggestion that the number of Si–Si bonds is free to adjust itself such that E_F remains in a minimum of the density of states [65].

Ab initio molecular dynamics calculations provide a more distinct picture [66]. The Si–Si–Si bond-angle distribution now displays a huge peak around 120°, much larger even than that around 60°. In contrast, the Li–Li–Li distribution has broader and lower maxima. This difference between the bond-angle distributions of the anions and the alkali ions reminds us of CsPb (figure 8). It reflects the covalent character of the Si–Si bonds. It is interesting to compare this to the results of a similar exercise for K–Si [67], where in the Si–Si–Si bond angle distribution the maximum at 60° is much more pronounced than the one at 110–120°, possibly because of the formation of Si_4 tetrahedra.

Alkali–Si and alkali–Ge alloys lend themselves to checking relationships between nuclear-magnetic-resonance properties and electrical conductivity, as first formulated by Warren [68], and derived more rigourously by Götze and Ketterle [69]. As this topic falls slightly outside the scope of this paper we refer to the relevant papers [65, 70, 71].

5. Liquid alkali–pnictide alloys

We have briefly noted that the alkali–tin alloys are very similar to the alkali–lead ones. This is understandable from the relative positions of the elements Pb and Sn in the periodic table. Such a close similarity does not exist for the alkali–bismuth and alkali–antimony alloys. Therefore the two alloy systems are treated separately. An instructive paper on the properties of the solid alloys has been written by Tegze and Hafner [72].

5.1. Alkali–antimony alloys

The phase diagrams of the alkali–antimony alloys exhibit congruently melting compounds A_3Sb for the octet compositions of all binary systems and for the equiatomic compounds of Na, K, Rb and Cs with Sb. In the latter the Sb atoms occur in spirals around nearly perfect fourfold screw axes. This configuration can be interpreted as a Zintl ion as it is comparable to the essentially one-dimensional helical chain configuration in tellurium [73].

The electrical conductivities of liquid Na–Sb and Cs–Sb have been measured by Redslob *et al* [74]. Later new data were published [75, 76], which in the concentration range around the octet compound show significant improvements over the former ones and include some data on K–Sb. The maximum resistivities are all in the semiconducting range.

Na–Sb exhibits a sharp conductivity minimum at 25% Sb, the octet composition [75]. The behaviour at Sb concentrations higher than 50% is not known. The Darken stability function has also a very sharp maximum at 25% Sb [76]. In K–Sb and Cs–Sb the minimum of the conductivity at the octet composition has become very shallow and gives way to a plateau-like one between 35 and 50% Sb [76]. As for Na–Sb the Darken stability function has maxima at 25% Sb, but its height decreases strongly in the direction Na–Sb, K–Sb, Cs–Sb [76]. Additional, broader maxima appear at 48% Sb for K–Sb and at 54% for Cs–Sb [76, 77].

Within Geertsma's model the phenomena around 50% can be interpreted as arising from polyanion formation, although the stoichiometric composition is not well defined. The Zintl compound is then the first candidate to consider. As it corresponds to an infinite chain it can not survive as such in the liquid. We must assume that the polyanions are broken up into fragments in the melting transition. Considerable evidence for this supposition comes from neutron diffraction experiments on a number of liquid Cs–Sb alloys [40]. We concentrate on the equiatomic compound. The structure factor displays a prepeak at $k_0 = 0.95$ Å^{-1}, which corresponds, using the rule of thumb $dk_0 = 7.7$ [40], to a superstructure with a characteristic length of 8 Å. This is, allowing for thermal expansion, in very good agreement (perhaps fortuitously so) with the interchain distance of 7.6 Å in solid CsSb. A peak at 2.83–2.84 Å in the radial distribution function is attributed to Sb–Sb nearest-neighbour distances within the chain. The corresponding covalent distance in the crystal is 2.85 Å (it is a general observation that the length of the covalent bond in a polyanion is affected relatively little by heating and melting). Finally, the Sb–Sb coordination number is found to be 2, which would be in agreement with the existence of infinite one-dimensional chains in the liquid. The actual length is not known, but chains as short as Sb_4, occurring in crystalline K_5Sb_4 [78], are probably ruled out within the limits of experimental accuracy.

It is an obvious suggestion to attribute the 'irregularities' found in the physical properties (the broadness of the minimum in the conductivity and the deviations from 50% of the positions of the maxima in D) to the occurrence of a variety of chain lengths, but such details have as yet to be sorted out. More particularly, there is room for supplementary investigations on the antimony-rich side of the phase diagram.

In this short account we have kept to the compositions where polyanion formation is suspected. Much research has been carried out on the solid and liquid octet compounds, first because they are interesting cases for studying electronic processes in (disordered) semiconductors and second, because the solid compounds are interesting starting materials for constructing photo-emitters. As examples of the first kind we mention, rather arbitrarily, [75] and [79].

5.2. Alkali–bismuth alloys

Like the alkali–antimony alloys, the alkali–bismuth alloys have congruently melting octet compounds, A_3Bi. Besides, and in contrast to the antimony systems, in K–Bi, Rb–Bi and Cs–Bi congruently melting compounds ABi_2 occur. Equiatomic compounds exist only as LT phases in Li–Bi and Na–Bi whereas for the other systems there is a eutecticum at this composition.

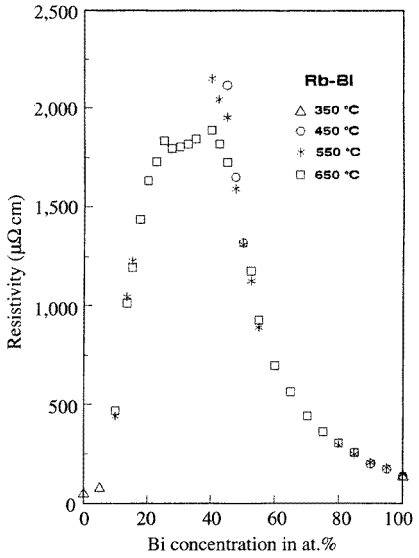

Figure 11. Resistivity of liquid Rb–Bi alloys as a function of composition and for temperatures indicated in the figure. (Reproduced from [81].)

The liquid alloys offer a confusing picture. The resistivity measurements show a very gradual transition from an octet compound for Li–Bi to a compound at 40% Bi for Cs–Bi [80–82, 12]. In the intermediate systems K–Bi and Rb–Bi peaks occur at both compositions (figure 11). The resistivity maximum in Cs–Bi is rather broad, suggesting that the stoichiometry is not well defined. Measurements of the Darken stability functions confirm the octet compound, but suggest a stoichiometry of 50% for the second compound in Na–Bi, K–Bi and Rb–Bi [83–85, 79].

So, as far as the second compound is concerned, there is a significant discrepancy

between the indications from thermodynamics and from resistivity measurements; additionally there seems to be no link with the phase diagram. The congruently melting compounds KBi_2, $RbBi_2$ and $CsBi_2$ do not show up in the physical properties of the liquid alloys. These are Laves phases in the solid state, just like KPb_2, which also is not discernible in the liquid (but which is not congruently melting). The assumption that, as in the antimony alloys, variable-size chain fragments are formed could be a starting point for understanding the stoichiometry problem.

It is remarkable that the behaviour of the alkali–bismuth alloys is so different from that of their alkali–antimony brothers. Such differences do not exist between Sn and Pb, and, as we will see, between In and Tl, though the positions of these pairs in the periodic system are comparable. It might be that the relativistic effects in the bismuth atom have a particularly strong influence on their bonding properties. This suggestion is also roused by recent *ab initio* calculations on the (nonclustering) compound Mg_3Bi_2 [86].

In K–Bi, Rb–Bi and Cs–Bi also the temperature derivative of the resistivity behaves peculiarly. At the 50% composition the resistivities are between 1000 and 2300 $\mu\Omega$ cm. One then expects a negative $d\rho/dT$ (see, e.g. the table in [6]), but the actual values are zero within the accuracy of the measurements.

Summarizing, the behaviour of the alkali–bismuth alloys is still puzzling and may form an interesting subject for further investigations.

6. Liquid alkali–tellurium alloys

A clear-cut example of Zintl ion formation is provided by liquid KTe. Liquid potassium–tellurium alloys have been the object of intensive studies by groups at Argonne and in Montreal. Their work is summarized in [87].

The stability function exhibits a very high and sharp maximum at 49% K [88], not significantly different from the equiatomic composition. This indication for compound formation could be confirmed only partly by resistivity measurements, which are, as yet, confined to potassium concentrations of 0–50%. Assuming complete charge transfer, at the equiatomic composition Te^- ions are formed, which are isoelectronic to the halogen atoms. According to the Zintl model the polyanions may assume the dumbbell shape of halogen molecules. Indeed, such dumbbells exist in solid KTe [87].

The assumption of such Zintl ions in the liquid phase was confirmed almost beyond doubt by diffraction measurements [89]. The Te–Te distance is 2.8 Å, to be compared to 2.789 Å in the crystal. The Te–Te coordination number is found to be 0.96, very close to unity as expected for dumbbells. Finally, the position of the prepeak according to [89] is at 1.2 $Å^{-1}$, which corresponds approximately to a distance of 6.4 Å in real space. This should be compared to the average distance between the centres of the dumbbells in the crystal, which is 6.2 Å.

Beside the sharp maximum in the stability function at 49% K there is a lower, but still distinct maximum at 12% K. For this composition the radial distribution function has a first peak at 2.78 Å, which is again attributed to Te–Te distances. From a more detailed analysis the authors conclude that Te chains of five to ten atoms persist in the melt.

In Na–Te solutions similar effects as in K–Te, though considerably weaker, were found [90]. Once more, the stability of the polyanionic configuration appears to be related to the size of the alkali atom in the way predicted by Geertsma's model.

7. Liquid alkali–group-13 alloys

Historically, LiAl and NaTl played an important role in the discovery of rules for Zintl ion formation [13, 91]. LiAl, LiGa, LiIn, NaIn and NaTl crystallize in the NaTl (B32) structure, consisting of two interpenetrating diamond lattices. Indeed, their band structures show a great deal of similarity with that of Si, but the gap is bridged [92]. This would make them interesting cases for investigation in the liquid state, but, as yet, they have not lived up to the expectations. The resistivities remain within the NFE regime, there are only broad and low maxima in the alkali-rich region of the resistivity–composition plots. It should be noted that also the solid equiatomic compounds are metallic. The alkali Knight shifts display stronger effects: they drop fast when the polyvalent metal is added to Li or Na. Probably there is considerable charge transfer resulting in some sort of ionic mixture, as in Li–Pb, but without the well defined stoichiometry of the latter. For the formation of an octet compound, five electrons have to be transferred to the polyvalent atom, and therefore on-site repulsion might be prohibitively strong.

In the liquid state we can expect at most fragments of the infinite Zintl ion (the diamond lattice) to exist, in analogy with the fragmented Te-like chains supposed to survive in liquid Cs–Sb. Indications for such behaviour, if any, are weak.

The behaviour of the resistivity changes markedly if one proceeds to the potassium, rubidium and caesium alloys. In this order, the resistivities of the alkali–In, Tl alloys rapidly become higher and peak up more sharply, with the maxima occurring at compositions very near to 50% (see figures 12 and 1). Still, the resistivities do not exceed 900 $\mu\Omega$ cm, which is low compared to the alkali–group-14, 15 and 16 systems [12, 29, 93–95].

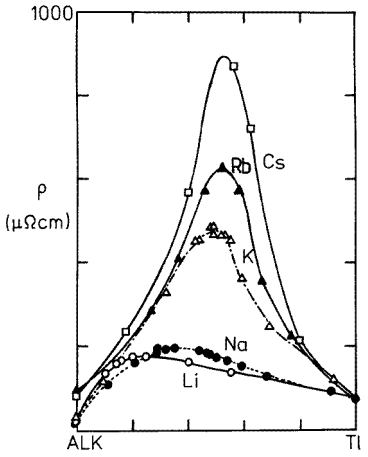

Figure 12. Resistivities of liquid alkali–thallium alloys as a function of composition. Temperatures: Li–Tl, 800 °C; Na–Tl, 310 °C; K–Tl, 340 °C; Rb–Tl, 653 °C; Cs–Tl, 420 °C. The figure is reprinted from Itami T, Izumi K and Iwaoka N 1993 *J. Non-Cryst. Solids* **156–158** 285–8 with kind permission from Elsevier Science-NL, Sara Burgerhartstraat 25, 1055 kV, Amsterdam, The Netherlands. The data for Li–Tl in [94] are adopted from [31].

Much more spectacular effects are observed in the neutron-diffraction data for liquid K–Tl and Cs–Tl alloys, which exhibit prepeaks at unusually small momentum transfers k_0, *viz.* 0.80, 0.70 and 0.68 Å^{-1} for KTl† [96], CsTl [96] and Cs_8Tl_{11} [97], respectively,

† In [96] a momentum transfer of 0.77 Å^{-1} was communicated due to an inaccurate reading of the graph.

corresponding to distances d in real space of 9.62, 11 and 11.3 Å (see figure 13). Such long-range structures are exceptional in liquid alloys.

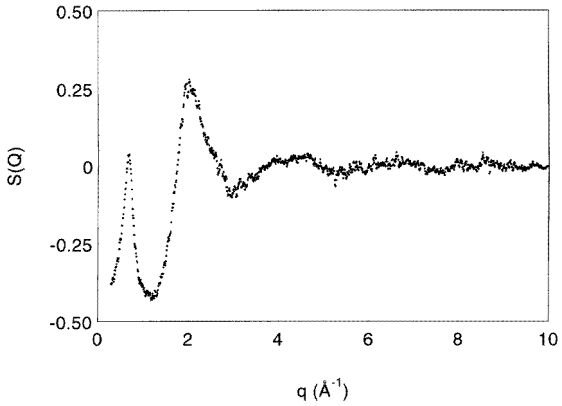

Figure 13. The structure factor of liquid Cs_8Tl_{11}. Unpublished data, still lacking the optimum refinement, obtained by Van der Aart, Verkerk, Badyal and McGreevy.

This observation almost coincided with the discovery of a rich variety of fascinating crystal structures in compounds of potassium, rubidium and caesium with indium and thallium. The unit cells contain compact anion clusters, in contrast to the more network-like diamond lattice configurations in the Li and Na compounds. An important group of compounds has the composition A_8B_{11}, in which A denotes K, Rb or Cs and B denotes In or Tl [98–101]. They are all isomorphous and contain large compact polyanions Tl_{11}^{8-} or In_{11}^{8-} (see figure 14). The chemical bonding in these units can no longer be understood from the valence rule (1), but is described in terms of a deviation from the Wade rules. The average distance d_s between the centres of the polyanions is 10.7 Å in Cs_8Tl_{11}, which compares favourably to the characteristic distance of 11.3 Å found in liquid Cs_8Tl_{11}. This suggests that polyanions similar to Tl_{11}^{8-} occur in the liquid. The number of atoms per cluster in the liquid should be considered with some reserve, as it scales with k_0^{-3}, as will be shown below.

The comparison of the liquid equiatomic mixtures KTl and CsTl with their solid counterparts does not reveal such strong similarities. The crystals contain Tl_6^{6-} polyanions with intercluster distances of 8.71 and 9.26 Å, respectively [102, 103]. These numbers differ significantly from the corresponding ones in the liquid, given above as 9.62 and 11.0 Å. Probably the clusters are larger in the liquid than in the solid (see the next section).

Later Sevov and Corbett discovered that stable polyanions are formed in ternary alloys of K, In and a transition metal. A most fascinating example is $Na_{96}In_{97}Pd_2$, which contains fullerene-type polyanions [104]. Another example is $K_{10}In_{10}Pd$, in which Pd-centred $PdIn_{10}$ polyanions occur ([105], see also figure 15). Experiments in the liquid state were carried out for $K_{10}Tl_{10}Pd$, which on empirical grounds is expected to be structurally almost undistinguishable from $K_{10}In_{10}Pd$ [106]. Compared to KTl, the prepeak position drops from 0.80 to 0.72 Å^{-1}, which corresponds to a distance in real space of 10.7 Å. The intercluster distance in crystalline $K_{10}In_{10}Pd$ is 10.5 Å. Once more the agreement is very satisfactory. The liquid obviously follows the trend in the solid state.

A great deal of the structural chemistry of the alkali–group-13 systems (and their ternary derivatives) has been discovered since 1990 and the field is still developing rapidly. The

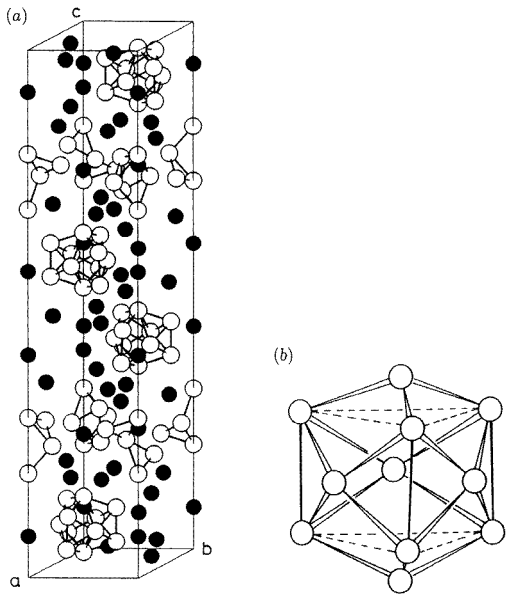

Figure 14. (*a*) The crystal structure K_8Tl_{11}: black points, K atoms; open circles, Tl atoms. (Reproduced from [96].) (*b*) The Tl_{11} cluster in K_8Tl_{11}. (Reproduced from [96].)

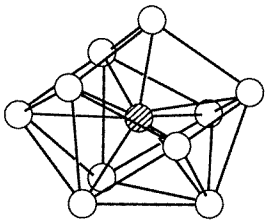

Figure 15. An $In_{10}Pd$ cluster in $K_{10}In_{10}Pd$ (an example; there are two kinds): shaded circle, Pd atom. (Reproduced from [105] in slightly modified form, with permission from the American Chemical Society.)

architectural richness is astonishing, the structures are unexpectedly long ranged. [9] gives many examples. That evidently remnants of these large-scale structures are preserved in their liquid testifies to the strength of the underlying bonding principles.

8. Conclusions

There can be little doubt that polyanions exist in the liquid ionic alloys discussed in the preceding sections. Arguments in favour of their existence are the shifts of the stoichiometric compositions, the sharp prepeaks in the structure factors, the similarity of the anion–anion bond lengths in the liquid and the solid and the distinct differences between the bond-angle distributions for the alkali ions and for the polyvalent metal ions, as found from *ab initio* calculations. Furthermore there exists some strong systematics.

First, Geertsma's stability rule is universally observed within the group of binary systems

discussed, much more than one may expect given the simplifications made in its derivation. There is room here for some further theoretical work.

Second, the relation between the structure of the liquids and that of their solid counterparts is strong. In the following we will elaborate on this latter point in a more quantitative way, thereby summarizing some scattered data from the preceding sections.

We have several times used the relation

$$k_0 d_l = 7.7 \tag{2}$$

where k_0 is the wavenumber corresponding to a superstructure peak in the structure factor and d_l is a distance in real space associated with k_0. In practice, d_l has been interpreted by us as an intercluster distance. The derivation of equation (2) is based on a comparison with diatomic molecules [40, 41]. The number 7.7 is obtained from calculating the spherical average of $e^{i\boldsymbol{q}\cdot\boldsymbol{R}}$, which has a first non-trivial maximum at $qR = 7.7$. Equation (2) should be considered as no more than a rule of thumb. More particularly the shape of the prepeak has not been considered [107] and alternative numbers have been proposed instead of 7.7 [108]. The arguments put forward in the following do not strongly depend on the precise value of this number.

In the preceding sections we have tacitly used the following formula for deriving an average intercluster distance d from crystallographic data:

$$d = 1.122\Omega^{1/3}. \tag{3}$$

Here $\Omega = V/N$, the volume per cluster, V being the total volume of the material considered and N the number of clusters in V. The relation (3) is obtained by putting the centres of the clusters on an fcc lattice as this stimulates best the isotropic structure of a liquid. It has been used to convert crystallographic data into average intercluster distances in a fictitious liquid with the same density as the crystal. It can be applied to a real liquid as well, provided Ω is known for the liquid phase.

We can now estimate the number of anions forming part of a cluster. If A is the number of single anions in V and n the number of anions in a cluster, $n = A/N$, and we may define a sort of effective volume per anion, $\omega = (V/A) = \Omega/n$. In this approximation n is considered to be equal for all clusters (in the liquid state this is only approximately so). Note that ω is not the partial atomic volume. We easily find

$$n = d^3/(1.4124\omega). \tag{4}$$

Also equation (4) can be applied to the liquid as well as the solid state.

We can now estimate the distances between clusters in the liquid with the help of (2) and compare them to average distances derived from the crystallographic data using (3). The result is shown in figure 16. We see that the relation between cluster distances in the solid and the liquid state is linear with a remarkable precision in a distance range of approximately 1:1.7. The slope of the dashed line is 1.04, the deviation from unity accounting approximately for the thermal expansion and the expansion during melting. To show the general applicability of (2) and (3) we have added two cases from far outside our present field of interest: the molecular liquid I_2 and liquid Na. In the latter, somewhat pathological case, each single Na atom was considered as a cluster and d_l was derived from the main peak.

The following qualifications pertain to the points in figure 16. In CsSb the Zintl ions in the solid are one-dimensional and d is an interchain, rather than an intercluster distance. Its value has been obtained directly from the crystallographic data. Liquid $K_{10}Tl_{10}Pd$ was compared to solid $K_{10}In_{10}Pd$, which has nearly equal lattice parameters. For expanded KPb a fictive solid was used as reference: a volume increase was applied proportional to

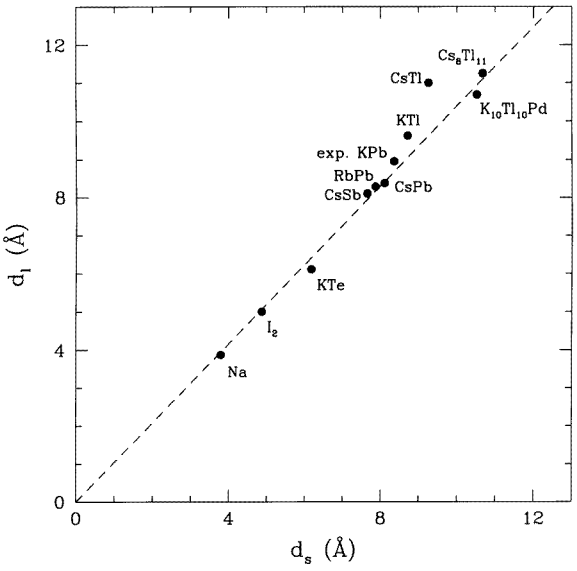

Figure 16. The characteristic distance in the liquid (d_l), calculated from equation (2), compared to the average intercluster distance in the crystal, d_s, according to equation (3). The dashed line is a least-squares fit to all the points except those for KTl and CsTl.

the expansion of the liquid between the melting point and the thermodynamic state of the measurement.

The points for KTl and CsTl are not well in line with the other data. Using the data of [96] for KTl would result in a point distinctly on the right-hand side of the straight line in figure 16. This is due, first, to the inaccuracy mentioned before and, second, to the fact that, for lack of data on crystalline KTl, unequal compositions were compared in [96]. Using equation (4) and calculating ω from [102] we estimate the number of atoms per cluster to be approximately eight whereas Tl_6^{6-} octahedra are found in crystalline KTl [102]. Note that n is very sensitive to errors in d. Therefore the parallelism between solid and liquid appears to be less than perfect for KTl and CsTl. This may be related to the large variety of (usually large) clusters found in this class of alloys, which makes any one-to-one correspondence between a liquid and a particular crystal structure somewhat illusory. For instance, Tl_{13} clusters have been recently discovered in mixed alkali–Tl compounds [109]. Still, figure 16 conveys an important message. The average intercluster distance and (neglecting for the moment variations in ω) the cluster size are almost independent of the state of order of the material, but are determined only by the chemical constitution. This is the more remarkable as in the liquid we had to allow for considerable deviations from the ideal polyanion structure (figure 7).

Related to this problem is the paradox of sharp features (prepeaks and stoichiometries) arising from strongly disordered systems. These sharp features survive remarkably well at high temperatures. It is as if an ionic charge density wave occurs in the liquid. There is a need for a more statistical description of polyanions in liquids, on the one hand accounting for general valence principles, on the other hand relaxing the proper Zintl–Klemm–Busmann concept or its Wade analogues. This constitutes a theoretical challenge.

There are also still plenty of experimental challenges: the bismuth alloys, further

investigations of the alkali–group-13 systems, extreme thermodynamic conditions and simply the filling up of still unexplored areas in the periodic table, such as the alkali–germanium alloys, which as yet have prohibited investigation because of serious experimental problems, and the transition-metal alloys. Some simple properties have been neglected by the experimentalists. For several systems phase diagrams are lacking or less than perfect; densities have to be guessed; atomic transport properties have hardly attracted attention. The determination of partial structure factors may be considered in some judiciously chosen cases. However for each individual alloy the efforts and costs invested in such an experiment should be weighted against the expected extra information. As we have seen, the total structure factor contains already the most important information: the range of the superstructure and the nearest-neighbour interatomic distances (the latter, indeed, by comparison with the crystalline data).

A decade has elapsed since the first firm experimental indications for polyanion formation were found [28, 40, 38, 29], but the field is still very much alive and there is still ample room for further investigations. Extrapolating the past, we may even hope for some surprises in the future.

Acknowledgments

The author would like to thank Dr P Verkerk for critically reading the manuscript and giving valuable advice. The author has benefitted from correspondence with Dr B Eisenmann on the limits of the Zintl ion concept. Dr G A de Wijs took care of figure 16. The author is indebted to S A van der Aart, Dr P Verkerk, Dr Y S Badyal and Dr R L McGreevy, and to Z-C Dong and Professor J D Corbett for making available as yet unpublished data on the liquid and solid thallium alloys, respectively.

References

[1] Tomlinson J L and Lichter B D 1970 *Metall. Trans.* **1** 305–7
[2] Mott N F and Davis E A 1979 *Electronic Processes in Non-crystalline Solids* (Oxford: Clarendon)
[3] Faber T E 1969 *Physics of Metals, 1. Electrons* ed J M Ziman (Cambridge: Cambridge University Press)
[4] Enderby J E and Barnes A C 1990 *Rep. Prog. Phys.* **53** 85–179
[5] Franz J R, Brouers F and Holtzhey C 1980 *J. Phys. F: Met. Phys.* **10** 235–52
[6] Allgaier R S 1969 *Phys. Rev.* **185** 227
[7] Fortner J, Karpov V G and Saboungi M-L 1995 *Appl. Phys. Lett.* **66** 997–9
[8] van der Marel C, Geertsma W and van der Lugt W 1980 *J. Phys. F: Met. Phys.* **10** 2305–12
[9] Kauzlarich S (ed) 1996 *Chemistry, Structure and Bonding of Zintl Phases and Ions* (Chemie) at press
[10] van der Lugt W and Geertsma W 1987 *Can. J. Phys.* **65** 326–47
[11] Saboungi M-L, Geertsma W and Price D L 1990 *Annu. Rev. Phys. Chem.* **41** 207–44
[12] van der Lugt W 1991 *Phys. Scr.* T **39** 372–7
[13] Zintl E and Woltersdorf G 1935 *Z. Elektrochem.* **41** 876–9
[14] Busmann E 1961 *Z. Anorg. (Allg.) Chem.* **313** 90–106
[15] Klemm W and Busmann E 1963 *Z. Anorg. (Allg.) Chem.* **319** 297–311
[16] Pearson W B 1964 *Acta Crystallogr.* **17** 1
[17] Wade K 1975 *Chem. Br.* **11** 177–83
[18] Shriver D F, Atkins P W and Langford C H 1991 *Inorganic Chemistry* (Oxford: Oxford University Press)
[19] Nesper R 1990 *Prog. Solid State Chem.* **20** 1–45
[20] Springelkamp F, de Groot R A, Geertsma W, van der Lugt W and Mueller F M 1985 *Phys. Rev.* B **32** 2319–25
[21] Brundle C R, Kuebler N A, Robin M B and Basch H 1972 *Inorg. Chem.* **11** 20–5
[22] Wang L-S, Niu B, Lee Y T, Shirley D A, Ghelichkhani E and Grant E R 1990 *J. Chem. Phys.* **93** 6318–26
[23] Geertsma W, Dijkstra J and van der Lugt W 1984 *J. Phys. F: Met. Phys.* **14** 1833–45
[24] Harrison W A 1980 *Electronic Structure and the Properties of Solids* (San Francisco: Freeman)

[25] Geertsma W 1990 *J. Phys.: Condens. Matter* **2** 8517–24
[26] Tegze M and Hafner J 1989 *Phys. Rev.* B **39** 8263–74
[27] Hart R R, Robin M B and Kuebler N A 1965 *J. Chem. Phys.* **42** 3631–8
[28] van der Marel C, van Oosten A B, Geertsma W and van der Lugt W 1982 *J. Phys. F: Met. Phys.* **12** 2349–61
[29] Meijer J A, Geertsma W and van der Lugt W 1985 *J. Phys. F: Met. Phys.* **15** 899–910
[30] Meijer J A, Vinke G J and van der Lugt W 1986 *J. Phys. F: Met. Phys.* **16** 845
[31] Nguyen V T and Enderby J E 1977 *Phil. Mag.* **35** 1013–9
[32] Ruppersberg H and Reiter H 1982 *J. Phys. F: Met. Phys.* **12** 1311–25
[33] Tumidajski P J, Petric A, Takenaka T, Pelton A D and Saboungi M-L 1990 *J. Phys.: Condens. Matter* **2** 209–20
[34] Saboungi M-L, Leonard S R and Ellefson J 1986 *J. Chem. Phys.* **85** 6072–81
[35] Saar J and Ruppersberg H 1988 *Z. Phys. Chem., NF* **156** 587–91
[36] Tumidajski P J 1991 *Can. Metall. Q.* **30** 271–3
[37] van der Marel C, Stein P C and van der Lugt W 1983 *Phys. Lett.* **95A** 451–3
[38] Alblas B P, van der Lugt W, Dijkstra J, Geertsma W and van Dijk C 1983 *J. Phys. F: Met. Phys.* **13** 2465–77
[39] Reijers H T J, Saboungi M-L, Price D I, Richardson J W Jr and Volin K J 1989 *Phys. Rev.* B **40** 6018–28
[40] Lamparter P, Martin W, Steeb S and Freyland W 1983 *Z. Naturf.* a **38** 329–55
[41] Richter H 1960 *Fortschr. Fys.* **8** 493–527
[42] Reijers H T J, Saboungi M-L, Price D L and van der Lugt W 1990 *Phys. Rev.* B **41** 5661–6
[43] Reijers H T J, van der Lugt W and Saboungi M-L 1990 *Phys. Rev.* B **42** 3395–405
[44] Stolz M, Leichtweiss O, Winter R, Saboungi M-L, Fortner J and Howells W S 1994 *Europhys. Lett.* **27** 221–6
[45] Reijers H T J, van der Lugt W, van Dijk C and Saboungi M-L 1989 *J. Phys.: Condens. Matter* **1** 5229–41
[46] Price D L, Saboungi M-L, de Wijs G A and van der Lugt W 1993 *J. Non-Cryst. Solids* **156–158** 34–7
[47] Gilde D 1956 *Z. Anorg. Chem.* **284** 142–3
[48] Saboungi M-L, Reijers H T J, Blander M and Johnson G K 1988 *J. Chem. Phys.* **89** 5869–75
[49] Howe M A and McGreevy R L 1991 *J. Phys.: Condens. Matter* **3** 577–91
[50] Stolz M, Winter R, Howells W S and McGreevy R L 1995 *J. Phys.: Condens. Matter* **7** 5733–43
[51] van der Lugt W and Winnink M 1993 *Physica* B **191** 217–9
[52] de Wijs G A, Pastore G, Selloni A and van der Lugt W 1994 *Europhys. Lett.* **27** 667–72
[53] de Wijs G A, Pastore G, Selloni A and van der Lugt W 1995 *J. Chem. Phys.* **103** 5031–40
[54] Hafner J 1989 *J. Phys.: Condens. Matter* **1** 1133–40
[55] Price D L, Saboungi M-L, Reijers R, Kearly G and White R 1991 *Phys. Rev. Lett.* **66** 1894–7
[56] Price D L and Saboungi M-L 1991 *Phys. Rev.* B **44** 7289–96
[57] Saboungi M-L, Fortner J, Howells W S and Price D L 1993 *Nature* **356** 237–9
[58] Price D L, Saboungi M-L and Howells W S 1995 *Phys. Rev.* B **51** 14 923–9
[59] Fortner J, Saboungi M-L and Enderby J E 1995 *Phys. Rev. Lett.* **74** 1415–8
[60] Price D L, Saboungi M-L and Howells W S 1995 *Physica* B **213 & 214** 547–51
[61] Böhm M C, Ramirez R, Nesper R and von Schnering H-G 1985 *Ber. Bunsenges. Phys. Chem.* **89** 465–81
[62] Xu R and van der Lugt W 1991 *Physica* B **173** 435–8
[63] de Jong P H K, Verkerk P, van der Lugt W and de Graff L A 1993 *J. Non-Cryst. Solids* **156–158** 978–81
[64] de Jong P H K, Verkerk P, de Graff L A, Howells W S and van der Lugt W 1995 *J. Phys.: Condens. Matter* **7** 499–516
[65] Meijer J A, van der Marel C, Kuiper P and van der Lugt W 1989 *J. Phys.: Condens. Matter* **1** 5283
[66] de Wijs G A, Pastore G, Selloni A and van der Lugt W 1993 *Phys. Rev.* B **48** 13 459–68
[67] Galli G and Parrinello M 1991 *J. Chem. Phys.* **95** 7504–11
[68] Warren W W 1971 *Phys. Rev.* B **3** 3708
[69] Götze W and Ketterle W 1983 *Z. Phys.* B **54** 49
[70] Xu R and van der Lugt W 1994 *Z. Naturf.* a **49** 1019–22
[71] Geertsma W and van der Marel C 1995 *J. Phys.: Condens. Matter* **7** 8867–76
[72] Tegze M and Hafner J 1992 *J. Phys.: Condens. Matter* **4** 2449–74
[73] Bradley A J 1924 *Phil. Mag.* **48** 477–96
[74] Redslob H, Steinleitner G and Freyland W 1982 *Z. Naturf.* a **27** 587–93
[75] Heyer H, Egan J J and Freyland W 1992 *Ber. Bunsenges. Phys. Chem.* **96** 962–6
[76] Bernard J and Freyland W *Proc. 9th Int. Conf. on Liquid and Amorphous Metals; J. Non-Cryst. Solids* at press
[77] Saboungi M-L, Ellefson J, Johnson G K and Freyland W 1988 *J. Chem. Phys.* **88** 5812–7

[78] Somer M, Hartweg M, Peters K and von Schnering H G 1991 *Z. Kristallogr.* **195** 103–4
[79] Egan J J 1985 *High Temp. Sci.* **19** 111–25
[80] Steinleitner G, Freyland W and Hensel F 1975 *Ber. Bunsenges. Phys. Chem.* **79** 1186–9
[81] Xu R, Kinderman R and van der Lugt W 1991 *J. Phys.: Condens. Matter* **3** 127–33
[82] Meijer J A and van der Lugt W 1989 *J. Phys.: Condens. Matter* **1** 9779–84
[83] Takeda S and Tamaki S 1990 *J. Phys.: Condens. Matter* **2** 10 173–82
[84] Petric A, Pelton A D and Saboungi M-L 1988 *J. Phys. F: Met. Phys.* **18** 1473–89
[85] Petric A, Pelton A D and Saboungi M-L 1988 *J. Electrochem. Soc.* **135** 2754–60
[86] de Wijs G A 1995 *Thesis* Groningen
[87] Saboungi M-L, Fortner J, Richardson J W, Petric A, Doyle M and Enderby J E 1993 *J. Non-Cryst. Solids* **156–158** 356–61
[88] Petric A, Pelton A D and Saboungi M-L 1988 *J. Chem. Phys.* **89** 5070–7
[89] Fortner J, Saboungi M-L and Enderby J E 1992 *Phys. Rev. Lett.* **69** 1415–8
[90] Petric A, Pelton A D and Saboungi M-L 1989 *Ber. Bunsenges. Phys. Chem.* **93** 18–24
[91] Zintl E and Dullenkopf W 1932 *Z. Phys. Chem.* B **16** 195–205
[92] Christensen N E 1985 *Phys. Rev.* B **32** 207–28
[93] van der Lugt W and Zu R 1992 *Recent Developments in the Physics of Fluids* (Bristol: Institute of Physics) p F249
[94] Itami T, Izumi K and Iwaoka N 1993 *J. Non-Cryst. Solids* **156–158** 285–8
[95] Itami T, Xu R and van der Lugt W 1993 *J. Alloys Compounds* **210** 37–41
[96] Xu R, Verkerk P, Howells W S, de Wijs G A, van der Horst F and van der Lugt W 1993 *J. Phys.: Condens. Matter* **5** 9253–60
[97] van der Aart S A, Verkerk P, Winter R and McGreevy R L private communication
[98] Sevov S C and Corbett J D 1991 *Inorg. Chem.* **30** 4875
[99] Blase W, Cordier G, Müller V, Häubermann U, Nesper R and Somer M 1993 *Z. Naturf.* b **48** 754
[100] Cordier G and Müller V 1992 *Z. Kristallogr.* **198** 281–2
[101] Dong Z-C and Corbett J D 1995 *J. Cluster. Sci.* **6** 187–201
[102] Dong Z-C and Corbett J D 1993 **115** 11 299–303
[103] Dong Z-C and Corbett J D private communication; *Inorg. Chem.* at press
[104] Sevov S C and Corbett J D 1993 *Science* **262** 880–3
[105] Sevov S C and Corbett J D 1993 *J. Am. Chem. Soc.* **115** 9089–94
[106] van der Aart S A, van der Lugt W, Verkerk P, Xu R, van der Horst F and McGreevy R L *J. Non-Cryst. Solids* at press
[107] Salmon P S 1994 *Proc. R. Soc.* A **445** 351–65
[108] Price D L, Moss S C, Reijers R, Saboungi M-L and Susman S 1988 *J. Phys. C: Solid State Phys.* **21** L1069–72
[109] Dong Z-C and Corbett J D 1995 *J. Am. Chem. Soc.* **117** 6447–55